Effect of asymmetric material entrance on lubrication in cold rolling

Tribology International 175 (2022) 107810

Contents lists available at ScienceDirect

Tribology International

journal homepage: www.elsevier.com/locate/triboint

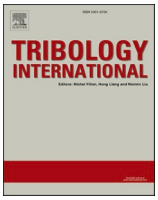

Effect of asymmetric material entrance on lubrication in cold rolling

L.J.M. Jacobs [a,c,*], K.N.H. van Dam [b], D.J. Wentink [c], M.B. de Rooij [a], J. van der Lugt [c], D.J. Schipper [a], J.P.M. Hoefnagels [b]

[a] Chair of Surface Technology & Tribology, Department of Mechanics of Solids, Surfaces & Systems (MS3), Faculty of Engineering Technology, University of Twente, 7500 AE Enschede, the Netherlands
[b] Department of Mechanical Engineering, Eindhoven University of Technology, 5600 MB Eindhoven, the Netherlands
[c] Tata Steel, Research & Development, 1951 JZ Velsen-Noord, the Netherlands

ARTICLE INFO

Keywords:
Cold rolling
Steel
Digital image correlation
Lubrication

ABSTRACT

An Integrated Digital Image Correlation (IDIC) method has been applied to the cold rolling process, the images clearly visualise the geometry of the roll bite and the inlet zone. A key, novel finding is that despite using coils and applying entry tension, the strip can enter asymmetrically in the rolling mill. Moreover, it is shown that asymmetric strip feeding results in an uneven lubricant film thickness between top and bottom strip surface. A method is detailed to feed the strip truly symmetrically in the mill, a procedure that is necessary for a meaningful experimental validation of lubricant film thickness models. For symmetric rolling processes the measured film thickness corresponds significantly better with the theory than for asymmetric processes.

1. Introduction

In the cold rolling process material is fed through a set of work rolls. By exerting force on these work rolls the material thickness is reduced. Due to the high speed and semi-continuous operation, the cold rolling process is the most widely used process in industry to reduce the thickness of steel sheet. From a tribological perspective, cold rolling is an interesting process because of the complex tribological behaviour in the roll bite [1]. This work provides a detailed analysis of lubrication and friction phenomena and in particular the effects of asymmetric strip feeding. Roberts [2] rightfully remarks that *"Of all the variables associated with rolling, none is more important than friction in the roll bite … its control within an optimum range for each process is essential*". It is well known that high friction results in high rolling force and rolling power, limiting mill capability. Other negative consequences are strip thickness variations and poor shape [3] or bad strip surface cleanliness [4]. Also, too low friction is detrimental to the rolling process: i.e. the motor power cannot be transmitted to the strip and 'skidding' occurs, possibly leading to uncontrolled vibrations [5], strip thickness oscillations [3] and again poor strip surface cleanliness [4]. However, not only the level of friction is important, friction must also be equally divided between upper and lower work roll. Jeng et al. [6] show how the amount of lubricant influences the roughness transfer and also the surface aspect of rolled strip, it can be deduced that asymmetric lubrication leads to surfaces with different visual aspect. Another problem, particularly for thin gauge strip rolling, is that asymmetric lubrication likely results in bow problems, i.e. a gradient in residual stress profile over the thickness of the strip [7]. It follows that control and regulation of friction are extremely important in cold rolling, for this purpose the process is always lubricated; [8] discusses a method for selection of cold rolling lubricants. However, not only the type of lubricant is critical, also the process conditions greatly influence the lubrication efficiency in cold rolling. From a lubrication point of view, a relevant geometrical aspect is the angle between strip and roll at the start of the contact, the so called "inlet angle" or "bite angle". The inlet angle has a direct influence on the rolling force as it influences significantly the lubricant film thickness that is entrained in the roll bite and consequently the friction between roll and strip, as shown by Wilson and Walowit [9] for rigid strip and work rolls. This monumental work has suscitated a lively interest in tribology based cold rolling models and these models have evolved enormously over the last 50 years. The influence of elastic deformation of work rolls has been investigated by Atkins [10], Lugt [11] describes a complete hydrodynamic rolling model where also elastic deformation of the strip is taken into account. Another major development is the transition from hydrodynamic rolling models to mixed lubrication models, for example by Marsault [12]. More recently, the focus has been on the transition of neat oil to emulsion lubrication: Wilson et al. [13] and Szeri

* Corresponding author at: Chair of Surface Technology & Tribology, Department of Mechanics of Solids, Surfaces & Systems (MS3), Faculty of Engineering Technology, University of Twente, 7500 AE Enschede, the Netherlands.
E-mail address: l.j.m.jacobs@utwente.nl (L.J.M. Jacobs).

https://doi.org/10.1016/j.triboint.2022.107810

Available online 25 July 2022

Nomenclature

Variables

b	Strip width (m).
D	Diameter guiding roll (m).
E	Young's modulus (Pa).
$\mathbf{E}$	Green-Lagrange strain tensor.
$\mathbf{F}$	Deformation gradient tensor.
h_{film}	Lubricant film thickness (m).
L	Length of strip-work roll contact (m).
P	Rolling force (N).
R_0	Work roll radius (m).
R'	Hitchcock deformed work roll radius (m).
t	Strip thickness (m).
U_{DIC}	Displacement following from DIC-analysis (m).
v	Speed (m/s).
$\mathbf{x}$	Eulerian position vector (m).
$\mathbf{X}$	Lagrangian position vector (m).
$\Delta x_{NP,exit}$	Distance neutral point to entry roll bite (m).
$\Delta x_{NP,entry}$	Distance neutral point to exit roll bite (m).
α	Inlet angle (rad).
η_0	Lubricant viscosity at atmospheric pressure and reference temperature (Pa·s).
γ	Pressure-viscosity coefficient (Pa^{-1}).
ν	Poisson ratio of work roll.
σ	Horizontal strip tension (Pa).
σ_{flow}	Flow stress of strip material (Pa).

Subscripts

x, y, z	Cartesian coordinates.
Roll	Work roll.
Strip	Strip material.
In/Entry	Entry side of roll bite.
Out /Exit	Exit side of roll bite.
NP	Position of neutral point.

Abbreviations

DIC	Digital Image Correlation.
IDIC	Integrated Digital Image Correlation.
ROI	Region Of Interest.

and Wang [14] describe lubrication mechanisms typical for emulsion lubrication and these are used by Cassarini [15] to formulate a complete model for emulsion lubrication that corresponds (at least qualitatively) with experimental observations. Boemer [16] provides a good overview of the state of the art of mixed-lubrication cold rolling models.

Experimental validation of a neat oil mixed-lubrication model is usually carried out with the droplet method, as first described by Azushima [17]. In contrast with the vast amount of literature on model development, experimental validation of these mixed lubrication models has received relatively little attention. In particular, while all mixed lubrication models indicate the importance of the inlet angle for lubrication, control of the inlet angle in the experimental validation of these mixed-lubrication models is not reported before. The droplet method simply assumes that the strip enters the roll bite in a symmetric way, i.e. the inlet angles with top and bottom surface are equal. However, Sutcliffe [18] carried out droplet trials on short strips and remarked that the strip tends to wrap around the unlubricated (bottom) work roll. If this happens, the inlet angle at the top surface significantly increases and consequently he measured thinner lubricant films than resulting from his (symmetric) model. It is therefore generally accepted that droplet trials are better carried out with coils (instead of small strips), as this allows the use of horizontal strip tension. Nevertheless, Aggerwal and Wilson [19] found that with small work rolls (50 mm diameter), the experimentally measured film thickness on coils was much bigger than the modelled film thickness. Cuperus et al. [20] used work rolls with 400 mm diameter (which is the approximate work roll diameter in a typical industrial 4-high mill), nonetheless they also measured thicker lubricant films than could be expected based on the model. The discrepancy in the experimental validation was always thought to be related to the accuracy of the cold rolling lubrication model. However a key step, the experimental proof that the strip truly enters the roll bite in a symmetric way, has so far never been studied in detail. In the current work this aspect is studied in detail.

Industrial interest in the cold rolling process has led researchers to develop models that are used by operators, researchers and scientists to better predict, analyse and understand the rolling process. Such models consist of modules that describe the elastoplastic strip deformation, the elastic work roll deformation and friction at the strip-roll interface. A comprehensive overview of different types of rolling models, their basic assumptions and their applicability is given by Montmitonnet [21]. Validation of rolling models is of great importance but due to their complexity, it is more convenient to validate the various sub-modules separately. For example, it is desirable to experimentally determine the exact contact geometry of the cold rolling process, such as the length of the strip-roll contact and the inlet angle. In the rolling model these features are directly related to the elastic work roll flattening module. Similarly the velocity fields within the deformation zone are directly related to the plastic strip deformation module. The validation of these sub-models, by experimentally determining the contact length and strip velocity gradients, is another objective of this work.

According to Montmitonnet [21], if the velocity gradients over the thickness are small, a slab model (or 1D-model) can be accurately used to describe the rolling process. In such a model the von Karman equation (resulting from force equilibrium) is solved to obtain the vertical pressure distribution in the contact zone [22]. The rolling force, usually the main outcome of a rolling model, is determined as the integral of the vertical pressure over the contact length. The contact length therefore has a significant influence on the rolling force.

Many different experimental methods have been employed by other researchers to measure the contact length between work roll and strip. The most straightforward method is to partly roll a piece of strip: after a fast mill stop, the shape of the contact is preserved and can be measured directly. This method has been employed by Sutcliffe and Rayner [23] on plasticine and Li et al. [24] for cold rolling of stainless steel. This method is only suitable to measure the plastic material deformation; during rolling, the geometry of the contact zone will be different due to the contribution of elastic strip deformation in the deformation zone.

Therefore, also in-situ methods have been developed to measure the contact length. An often used method is the 'inserted pin'-method in which a block with a pin protruding through the surface is integrated in a work roll, see for example Siebel and Lueg [25] for rolling of lead or Al-Salehi et al. [26] for rolling of steel, copper and aluminum. Stresses on the pin are measured with strain gauges or piezo-elements, so with this method not only the length of contact is measured but also the vertical stress and shear stress in the roll bite. Other, indirect, methods are to place strain gauges below the roll surface and use a model to deduce the stresses at the surface (Weisz-Patrault et al. [27]), to use ultrasound waves (Carretta et al. [28]), or to use the stress sensitivity of the reflected wave length of Bragg fibre gratings (Weisz-Patrault et al. [29]). A possible issue with all these methods is a limited resolution because of the finite dimensions of the measurement device. In this work the geometry is captured in-situ with a camera, this allows an accurate quantitative determination of the contact length and a qualitative evaluation of the inlet angle.

Different methods also exist to measure the deformation gradients in rolling. A commonly used method is to roll a piece of strip with an embedded pin, as done in Das et al. [30]. By comparing the shape of the pin after rolling with model results, velocity gradients and an average Coefficient of Friction over the contact length can be deduced. A higher accuracy can be obtained if a grid is made on the embedded insert, which also allows to stop the rolling process with the grid partly rolled as shown in Boldetti et al. [31]. Another advantage of these methods is that the deformation in the strip center can be measured, where the rolling process is plane strain. Both above methods are applied for hot rolling, but for cold rolling the velocity gradients over the strip thickness are much smaller and the methods are not accurate enough. The desired accuracy can be achieved with Digital Image Correlation (DIC), a contactless full-field measurement technique that can visualize both the contact geometry as well as velocity and strain gradients. DIC is a commonly used technique to visualize the deformation of solids in many different kind of processes; it can be applied relatively easily, based on regular images of the specimen surface. DIC has already been employed to visualize the deformation zone in cold rolling by Li et al. [32].

Another advantage of DIC is that the velocity gradients provide information about the position of the neutral point. The neutral point is an important concept in cold rolling theory, it is the position in the roll gap where the local strip speed is equal to the roll surface speed. In Li et al. [32] so called "Local DIC" is employed, velocity and strain field are determined based on two subsequent images of the rolling process. The fact that rolling is a steady state process is not exploited in this method. In the current work a recently developed, dedicated, IDIC framework for recurring material motion is employed that uses multiple images to accurately measure the velocity and strain fields during cold rolling. The method is described in detail in Hoefnagels et al. [33], the main advantage over local DIC is an improved accuracy and higher robustness. This technique is applied to visualize and analyze the cold rolling process on a pilot mill.

Despite the experimental and modelling effort of various researchers it must be concluded that the current accuracy of mixed lubrication models is not good enough for inline use as a setup model. A more accurate, validated, lubrication model for cold rolling would advance the steel industry to a higher level of process control. The present work offers important insights into the geometry of the strip, notably the inlet angle and the length of contact with the work rolls, as well as the velocity gradients inside the roll bite which enable to locate the position of the neutral point. This has not been studied before in such detail. In this work, for the first time, asymmetry with which the strip enters the rolling mill is measured in detail. Moreover, this study reveals the conditions under which the strip enters the roll bite in a truly symmetric way, which is a necessary condition for a meaningful validation of mixed-lubrication models. Both the first stand and later stands of a tandem mill are experimentally reproduced. It will be shown that there is a distinct difference related to the feeding of the strip in these stands.

The current manuscript is organized as follows: Section 2 describes the rolling theory that is necessary to interpret the experimentally achieved results. In Section 3 the experimental setup is detailed and the results are described in Section 4. Section 5 discusses the employed IDIC-method, the observed asymmetric material entrance and the relevance for industrial cold rolling mills. In Section 6 the conclusions of the work are summarized.

2. Theoretical background

Rolling models that neglect velocity, stress and strain gradients over the thickness and width could be considered a 1D-model. Such 'slab models' as firstly described by Orowan [34] neglect any shearing in the material, so the principal stress/strain axes remain the rolling direction, vertical direction and transversal direction. According to Montmitonnet [21] these methods give accurate results when the length of contact divided by the strip thickness is greater than 3, as is usually the case in cold rolling.

A description of elastic work roll deformation is an indispensable part of any cold rolling model. Due to elastic work roll deformation the contact length between roll and strip increases and therefore also the rolling force increases. In a slab model the elastic work roll deflection is coupled with the (elasto)plastic strip deformation. Convergence can typically be obtained by iteratively applying these two modules. Elastic deformation is complicated in nature, as any point force exerted on an elastic body impacts the deformation over the entire body (see for example Johnson [35]), but it can be implemented in a rolling model as in Jortner et al. [36]. An often made, accurate, assumption for cold rolling is that the work rolls remain circular in the contact zone albeit with a greater effective radius R' that is estimated by the following equation from Hitchcock [37]:

$$R' = R_0 \bullet \left(1 + \frac{16 \bullet (1-\nu_{roll}^2)}{\pi \bullet E_{roll}} \bullet \frac{P}{b \bullet (t_{in} - t_{out})}\right) \tag{1}$$

In this equation, t_{in} is the strip entry thickness, t_{out} the strip exit thickness, P the rolling force, b the strip width, R_0 the original work roll radius and $\upsilon_{roll}, E_{roll}$ are the elastic constants (Poisson ratio and Young's modulus) of the work roll material.

A schematic overview of the geometry around the contact zone is shown in Fig. 1.

With the assumption of locally circular work rolls, neglecting elastic strip recovery and by using simple geometrical relations, relevant parameters such as the contact length L and the inlet angle α and can be obtained from:

$$L = \sqrt{R' \bullet (t_{in} - t_{out}) - 0.25 \bullet (t_{in} - t_{out})^2} \approx \sqrt{R' \bullet (t_{in} - t_{out})} \tag{2}$$

$$\sin(\alpha) = \frac{L}{R'} \quad \text{which can be simplified to:} \quad \alpha \approx \sqrt{\frac{(t_{in} - t_{out})}{R'}} \tag{3}$$

The neutral point is an important concept in cold rolling. It is defined as the position in the contact zone where the horizontal strip speed equals the horizontal part of the roll speed. As cold rolling is considered to be a plane strain process, the assumption of locally circular work rolls also defines the strip speed in the deformation zone. Given a certain strip exit speed and a certain roll speed, the horizontal position of the neutral point can easily be expressed in terms of the deformed work roll radius:

$$\Delta x_{NP,exit} \approx \sqrt{R' \bullet (t_{NP} - t_{out})} \approx \sqrt{R' \bullet \left(\frac{v_{out} \bullet t_{out}}{v_{roll}} - t_{out}\right)} \tag{4}$$

$$\Delta x_{NP,entry} = L - x_{NP,exit}$$

In this equation, $\Delta x_{NP,exit}$ is the distance from the neutral point to the exit of the roll bite, $\Delta x_{NP,entry}$ the distance from the neutral point to the entry of the roll bite, t_{NP} the strip thickness at the neutral point, v_{out} the exit speed of the strip and v_{roll} the circumferential work roll speed. The objective of the IDIC-experiments described in this paper is to measure L, α and $\Delta x_{NP,exit}$, in order to validate the corresponding cold rolling theory.

In this work, IDIC is applied to the cold rolling process as described in Hoefnagels et al. [33]. In essence, DIC determines displacement fields by comparing two subsequent images. From the displacement fields, the deformation gradient tensor $\mathbf{F}$ can be determined:

$$\mathbf{F} = \frac{\partial \mathbf{x}}{\partial \mathbf{X}} \tag{5}$$

Here $\mathbf{x}$ is the Eulerian position vector and $\mathbf{X}$ the Lagrangian position vector, the derivatives in Eq. (5) are made with respect to the initial coordinates (Lagrangian approach). The determinant of the deformation gradient tensor yields the relative change of volume with respect to the initial state:

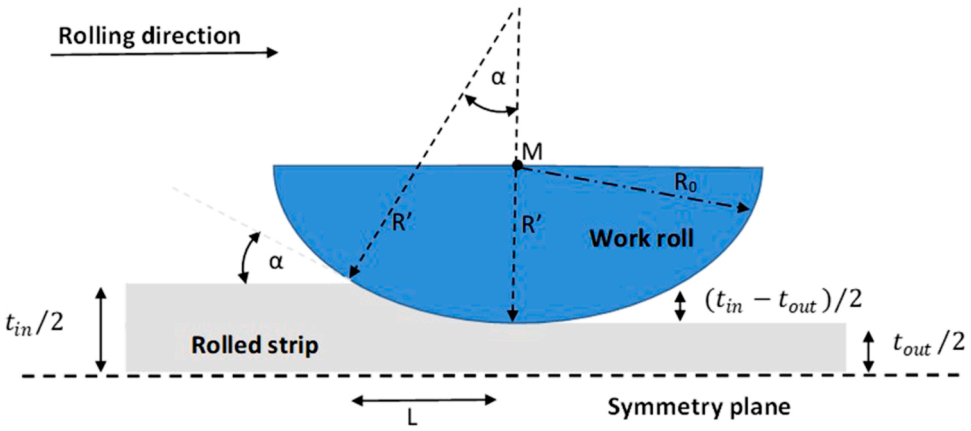

Fig. 1. side view of the strip-roll contact geometry (schematic) with the definitions of the parameters used in Eqs. 1–3. For clarity the various parameters are not properly scaled, only the part above the symmetry plane is displayed, only the lower part of the work roll is shown and the vertical deformation is highly exaggerated. M indicates the position of the work roll axis.

$$\det(\mathbf{F}) = \frac{V}{V_0}\left(\text{or, for a plane strain process such as cold } \textit{rolling}: \ \det(\mathbf{F}) = \frac{A}{A_0}\right) \tag{6}$$

Here V is the volume of a material element in the deformed state while V_0 is its volume in the undeformed state (in the 2D-equivalent, A is the surface of the element). As cold rolling is, by good approximation, a plane strain process it is expected that $\det(\mathbf{F}) \approx 1$, while values slightly smaller than 1 correspond to strip widening and values slightly higher than 1 correspond to strip narrowing.

The strain measure used throughout this article is the Green-Lagrange strain tensor $\mathbf{E}$, which is related to the deformation tensor by:

$$\mathbf{E} = \frac{(\mathbf{F}^{\mathrm{T}}\mathbf{F} - \mathbf{1})}{2} \tag{7}$$

Where $\mathbf{1}$ is the unity tensor.

3. Experimental set up

The pilot mill and DIC-setup are detailed in Section 3.1. The used material is detailed in Section 3.2 while the applied process variations are described in Section 3.3. Finally, Section 3.4 details the procedure to extract the contact length and neutral point position from the DIC-images.

3.1. Pilot mill and set up of DIC-experiment

The rolling experiments are carried out on a pilot mill of Tata Steel, see Fig. 2 for a photo and a schematic presentation. This stand-alone mill is capable of rolling coils up to 300 mm wide. Entry and exit tension are generated by the uncoiler and coiler. A set of guiding rolls is used to bring the strip at the pass line level, these rolls also measure strip speed and strip tension.

In the experiments the mill is operated in two-high configuration (i.e. without backup rolls). The work rolls with 393.4 mm diameter are ground to an R_a-value of 1.2 μm. A few coils were rolled before the actual experiment to wear off the work roll roughness peaks, this decreased the R_a-value to 0.9 μm.

Fig. 3 shows a schematic overview of the experimental DIC-setup and a photo of the camera and lighting inside the mill. The camera is a Basler scout scA1400–30gm with a resolution of 1392 × 1040 pixels. The maximum possible frame rate during the experiments was 25 frames per second. The desired working distance of 130 mm was achieved by equipping the camera with an appropriate lens system. A dedicated

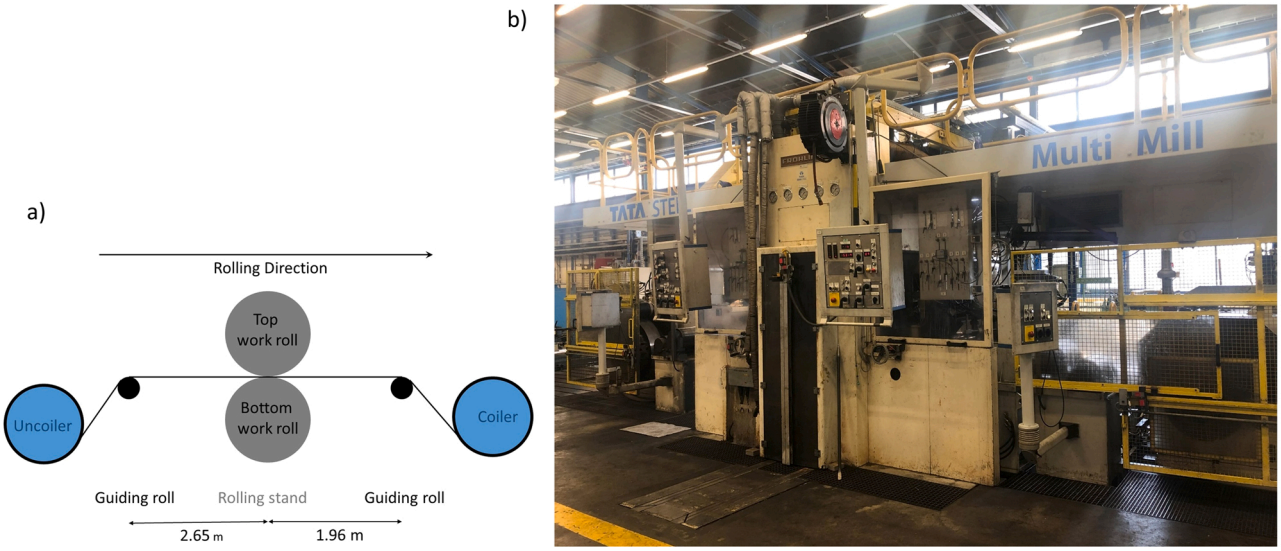

Fig. 2. experimental rolling mill: a) schematic layout, b) photo.

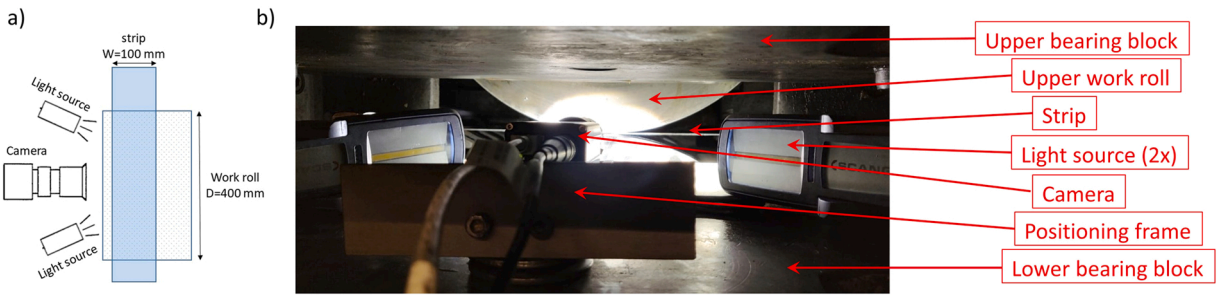

Fig. 3. experimental setup DIC-experiment. a) schematic overview seen from the top, b): side view photo of the setup between the two bearing blocks with view on the rolled strip.

positioning frame has been added to robustly fixate the camera onto the lower bearing block while it allows to conveniently bring the side of the strip in focus. For sharp images it was determined that one pixel corresponds with 15.6 μm. The lighting was provided by two LED-lights from the side.

Parameters measured during each rolling experiment were the entry strip speed, the exit strip speed, the work roll speed, the strip entry tension, the strip exit tension and the rolling force.

To guarantee sufficient lighting at the strip edge, the strip must be rolled off centric as schematically shown in Fig. 3a. The installed strip exit thickness measurement cannot be used for this extreme transversal position of the strip. The strip exit thickness is therefore deduced from the measured strip speeds and the known strip entry thickness by using mass conservation. Assuming material incompressibility and plane strain deformation yields:

$$t_{out} = t_{in} \bullet \frac{v_{in}}{v_{out}} \tag{8}$$

Two types of experiments were conducted:

1. Simulation of the first stand of a tandem cold rolling mill. In these tests the strip is passed directly from the uncoiler over the guiding roll to the roll gap. It will be shown later that bending over the guiding roll introduces residual stress in the steel strip, causing the strip to be fed asymmetrically in the mill.
2. Simulation of a later stand of a tandem cold rolling mill. In these tests the first pass is rolled in the same way as described above. The strip rolled in the first pass is then wound back and rolled again in a second pass. It is important to underline here that the piece of the strip that is rolled in the second pass has not passed over any guiding rolls after being rolled in the first pass, hence no residual stresses are introduced after rolling the first pass. Fig. 4 graphically presents this procedure, it will be shown that this procedure results in a truly symmetrical rolling process. The high acceleration rate of the mill assures the experiment is conducted well within the regime of stable rolling conditions.

3.2. Material rolled

The material used for the trial was a typical Interstitial Free steel grade with hot rolled thickness of 3.04 mm. The coil was produced via the normal steelmaking route up to cold rolling, then the material was slit in coils of 100 mm wide so that it could be used on the pilot mill. An approximate stress-strain curve is shown in Fig. 5, this curve is obtained from the internal database of Tata Steel, it is the average stress strain curve for this type of material. Surface roughness of the material before the first pass is characterised by an R_a-value of 1.5 μm.

Before rolling, the strip side edge was sprayed with graphite powder. This has no influence on the rolling process but it is done to provide contrast that is necessary for DIC. These graphite spots can clearly be seen in photos of the strip during processing (e.g. in Figs. 6, 8 and 10).

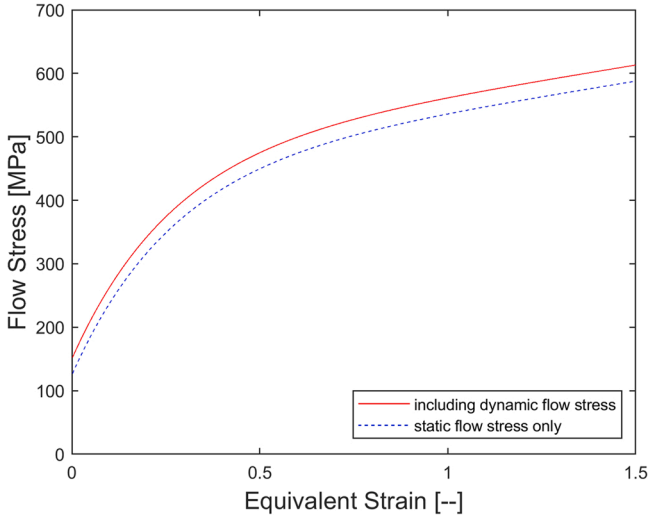

Fig. 5. expected stress-strain curve of strip material used in the experiment. Contribution of dynamic strain hardening is calculated for the reference process (as described in Section 3.3).

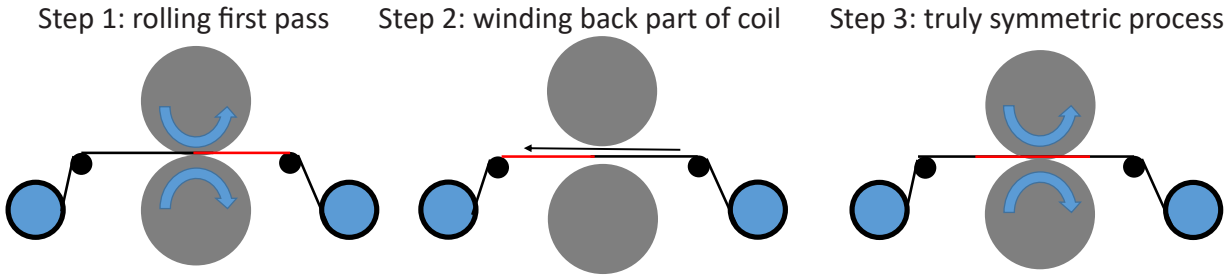

Fig. 4. visual presentation of the method to achieve a truly symmetric rolling process on the red part of the coil.

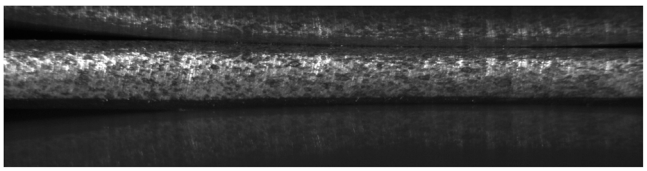

Fig. 6. image of strip for the reference process.

3.3. Overview of process variations

Rolling processes with different settings were carried out. A reference process was defined for which the entry tension force was 10 kN, the exit tension force 20 kN, the rolling force 750 kN and the rolling speed 10 mm/s. The rolling speed is significantly lower than in industrial rolling processes, which is necessary to limit the material transport between subsequent images in order to facilitate DIC. Nevertheless it will be shown below that, despite the low rolling speed, much can be learned about the industrial rolling process.

An overview of process deviations with respect to the reference process is given in Table 1. The variations in rolling force were mainly performed to achieve a wide range in observed contact length, while the variations in tension were mainly performed to achieve a wide range in observed neutral point position. Therefore these variations allow a validation of theory using IDIC-experiments. Two rolling passes were carried out, both with the same set of variations. When the IDIC-experiment was carried out on a second pass, the first pass was rolled with the reference settings. Only for the second (symmetrical) pass it is possible to make a comparison of contact length and position of the neutral point with the theory described in Section 2. The 1st pass variations were used to validate the IDIC-methodology and are detailed in Hoefnagels et al. [33], in this paper also the robustness and accuracy of the IDIC-method are described.

No coolant or lubrication was used, although the trial was started with work rolls wetted by a lubricating oil. The mill is rolling force controlled, hence the achieved strip exit thickness is the resultant of the other process settings and the friction during rolling. The achieved strip exit thickness varies therefore from process to process, it can even be different if all other process parameters are equal because the initially applied lubricant was gradually removed from the work roll. As a result the strip entry thickness before pass 2 varied (see Table 1), however this has no further influence on the resulting conclusions.

3.4. Extraction of relevant rolling parameters from the images

A typical image from the rolling process is shown in Fig. 6. The two work rolls and the strip (with speckle pattern) are visible, but despite optimised lighting, the image still has a low brightness level and a poor contrast (Fig. 10 shows the same photo with adapted contrast). Nevertheless, the image quality suffices to execute the IDIC-analysis on images similar to Fig. 6, but only after applying a mask [33] to assure that solely the strip is used for the DIC-calculation (and not the fixed parts of the

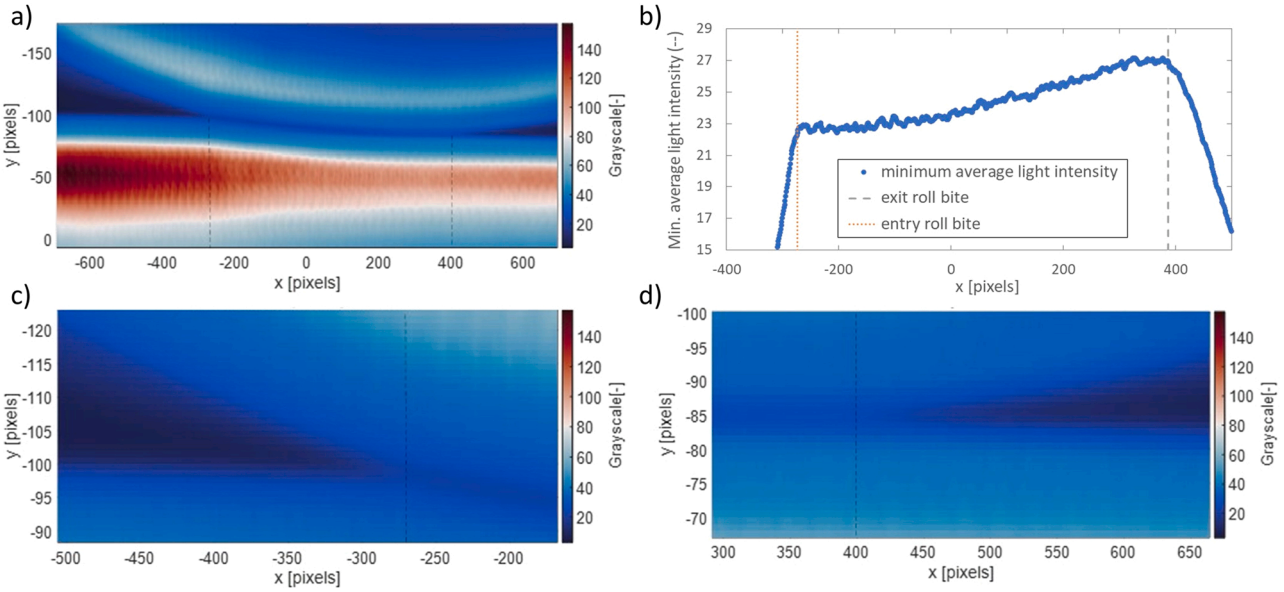

Fig. 7. visualisation of relevant steps to determine the contact length. a) average light intensity plot of 20 consecutive images, b) minimum value of the light intensity, c) zoom-in entry of roll gap, d) zoom-in exit of roll gap. The vertical dashed lines in all figures indicate the resulting position of the roll bite entry and exit.

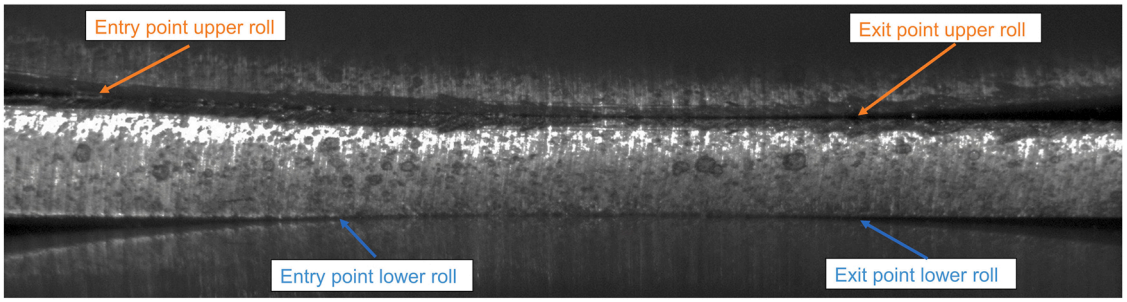

Fig. 8. photo of contact (contrast changed for clarity). Strip feeding conditions are similar to the first pass of a tandem mill.

Table 1
overview of experiments and the deviation of process conditions in each experiment with respect to the reference process. Entry thickness can vary slightly because of conditions in the first pass.

Experiment nr.	Strip entry thickness of 2nd pass (mm)	Deviation compared to reference process
1	2.23	Reference process (2x)
2	2.23	Rolling force 1000 kN
3	2.23	Rolling force 500 kN
4	2.23	Rolling force 1250 kN
5 *	2.40	Reference process
6	2.40	Rolling force 1250 kN
7	2.40	Entry/exit tension 10 kN / 10 kN
8	2.40	Entry/exit tension 10 kN / 30 kN
9	2.40	Entry/exit tension 15 kN / 15 kN
10	2.46	Reference process
11	2.46	Entry/exit tension 20 kN / 10 kN
12	2.46	Entry/exit tension 30 kN / 10 kN
13	2.46	Rolling speed 0.02 m/s

* In this article, all example photos and result graphs for the symmetric process are taken from the 5th process.

mill or the rotating work rolls).

In order to determine the contact length in an objective way, the average light intensity plot of 20 subsequent images (while running the mill) is used. The average light intensity per pixel is shown in Fig. 7a, with again the upper work roll, the strip and the gap between these two clearly visible. In Fig. 7a only the upper work roll is shown; this part of the rolling process is used for the analysis of geometry of the cold rolling process, as the lower work roll can obstruct the view on the bottom side of the strip in some cases.

Fig. 7a shows that the bigger the gap between work roll and strip, the lower the light intensity in the gap. The minimum value of the averaged light intensity (per horizontal position) can therefore be related to the gap height at that horizontal position. In Fig. 7b the minimum averaged light intensity is plotted against the horizontal position, the sharp increase of the minimum light intensity at the left of the graph can be read as 'narrowing of the gap'. Consequently it can be assumed that the entry of the roll bite is located at the position where the slope of this line changes sharply. For the exit a similar reasoning is made. In Fig. 7b, the position of the roll bite entry and exit are shown. Fig. 7c and Fig. 7d zoom in on the gap between roll and strip around the entry and exit of the roll bite. It can be verified that the position found with this algorithm corresponds to what would be found intuitively.

Applying the IDIC framework for steady-state material motion to 20 subsequent images gives the average displacement field between two subsequent images as explained in Hoefnagels et al. [33]. In order to relate this to strip speed, the displacement at the entry respectively exit is related to measured strip speeds:

$$v_{in} = C_{in} \bullet U_{x,DIC\_in} \tag{9}$$

$$v_{out} = C_{out} \bullet U_{x,DIC\_out}$$

Where U_{x,DIC_in} and U_{x,DIC_out} are the horizontal displacements following from the IDIC-analysis (at entry respectively exit), v_{in} and v_{out} are the measured strip speeds and C_{in} and C_{out} correction factors. An average correction factor is obtained by averaging C_{in} and C_{out}. The average correction factor could also be determined based on the approximated frame rate of the camera (25fps), the factor obtained with Eq. (9) corresponds within a few percent to this value. The horizontal displacements from the IDIC-analysis are corrected by the average correction factor to obtain the strip speed in the roll gap. The corrected speed can then be compared with the work roll speed to determine the position of the neutral point.

4. Results

Section 4.1 describes the strip-roll contact geometry for a rolling process for which the strip has moved over a guiding roll before being rolled. The impact of the resulting asymmetric material entrance is shown in Section 4.2. For a truly symmetric rolling process the validation of contact length and position of the neutral point is done in Section 4.3.

4.1. Observation of asymmetric strip feeding

A surprising result was that when material was rolled directly from the uncoiler over the guiding roll into the mill, the strip systematically entered the mill in an asymmetric way. This asymmetry cannot be observed with the naked eye, but it was clearly captured in the full-field measurement. An image of such a rolling process, for the reference process settings, is shown in Fig. 8.

In Fig. 8 the points where the rolls and strip come in contact are visually estimated and indicated with arrows. There is a clear asymmetry which is consistent over all these rolling trials. The strip arrives under an angle from above, consequently the strip always makes contact with the upper work first. The inlet angle in Fig. 8 is clearly smaller for the top work roll compared to the bottom work roll. It should be remarked that the strip always exits the roll bite in a symmetric way, as in Fig. 8.

As mentioned before, Sutcliffe [18] carried out droplet trials with short strips instead of coils and remarked that the strips tended to deflect at the roll bite entry, in his case increasing the top inlet angle. In this work it is demonstrated that asymmetric material entrance can even play a role when rolling coils while applying entry tension.

The root cause of this asymmetric material entrance was clearly established by comparing the material entrance for a few experiments. If exactly the same rolling experiment is repeated, but the strip material has not passed over any guiding roll before entering the mill (as in a second rolling stand experiment) the asymmetric behavior is not observed (see Fig. 10a). Furthermore it was shown that the asymmetry can also be invoked in the second pass, if again the material is passed over the guiding roll before rolling. From these observations it can definitely be concluded that the asymmetry is related to the passing of material over the guiding rolls, most likely because of the residual stresses introduced in the strip.

4.2. Influence of asymmetric strip feeding on lubrication

Section 4.1 shows that if a strip moves over a guiding roll before rolling, it enters the roll bite in an asymmetric way and the inlet angle with the top strip surface is smaller than with the bottom surface. The inlet angle is particularly relevant when considering lubricant flow. The well-known equation by Wilson and Walowit [9] demonstrates that smaller inlet angles result in thicker oil layers:

$$h_{film} = \frac{3 \bullet \eta_0 \bullet \gamma \bullet (v_{roll} + v_{out})}{\alpha \bullet (1 - e^{-\gamma(\sigma_{flow} - \sigma_{entry})})} \tag{10}$$

Where h_{film} is the lubricant film thickness at the bite entry, η_0 is the lubricant viscosity at atmospheric pressure and reference temperature, γ the viscosity-pressure coefficient as defined by Barus [38], σ_{flow} the material yield stress and other parameters have been defined before, notably the inlet angle α.

In order to examine the influence of asymmetric strip feeding on lubrication an extra pilot mill trial was carried out. A well-known test to experimentally determine the oil layer thickness is the droplet test, first reported by Azushima [17]. This method consists of rolling an oil droplet of a known volume that was placed in the strip center and after rolling

the area of the resulting spot is measured. The average oil film thickness at the exit of the bite is determined by taking the quotient of the volume and that area. Cuperus et al. [20] have compared several methods to experimentally determine the lubricant film thickness during cold rolling. They conclude that the droplet method gives the best results (in terms of precision and reproducibility). It is thus not surprising that this method is the most widely used to validate lubricant film thickness models and it was also chosen in the current work to demonstrate the difference between symmetric and asymmetric strip feeding conditions.

Two droplet test series were carried out, with two different lubricating oils. For these droplet tests, that were carried out after the IDIC-trials, material of other dimensions and steel grade was used. An overview of all relevant process, strip and oil parameters is given in Table 2. In each droplet test the rolling speed was varied as this parameter has a clear influence on the lubricant film thickness, so it allows for a good comparison of symmetric and asymmetric strip feeding conditions. No manifest shape defects were observed during the droplet tests.

In order to determine the influence of asymmetric feeding on the film thickness, in each test two types of rolling processes were performed (some tests were repeated to increase statistical significance). For the first process, the strip was fed over the guiding roll before being rolled, while in the second process the strip was not fed over any guiding roll before being rolled, as graphically shown in Fig. 4. Other test conditions were exactly equal between the two variants of each test. The measured film thickness at the exit of the roll bite is given in Fig. 9, as is common for these type of graphs, the log-log scale is used.

Fig. 9a shows the repeatability and robustness of the droplet method. For each process setting, the experiment was repeated 4 times and all results are shown in Fig. 9a. The standard deviation in film thickness for one process setting ranged between 5% and 9% of the average lubricant film thickness. The experiments in Fig. 9b were not repeated, but the linear relation between $\log(v)$ and $\log(h_{film})$ again shows that the measurement accuracy of the droplet trials is high.

To stress the impact of the guiding roll on the feeding conditions, the series in Fig. 9 are named “symmetric feeding” when the strip has not passed over the guiding roll before being rolled and “asymmetric feeding” when the strip has passed over the guiding roll before being rolled. The measured film thickness is consistently lower when the strip is fed symmetrically in the roll bite. This is consistent with the theory, the droplet is always placed on the top surface of the strip and the inlet angle with the top surface increases when the strip is fed straight in the mill. The difference between symmetric and asymmetric strip feeding can be significant: for the 1.40 mm material the lubricant film thickness for symmetric feeding is only half of the lubricant film thickness for asymmetric feeding. It can also be concluded that for thicker strip material the difference in film thickness is more important. According to Eq. (10), the inlet angle is inversely proportional to the film thickness, therefore it can be concluded that in these experiments the inlet angle was up to 100% larger for a symmetric rolling process. This corresponds to Fig. 8 showing a top inlet angle that is approximately a third of the bottom inlet angle.

These droplet trials show that asymmetric strip feeding not only occurs at extremely low rolling speeds (as in the DIC-trials), but also at higher rolling speeds. Furthermore, the droplet trials show that the observed asymmetry with DIC is not an edge effect (maybe caused by bad strip shape), but also the strip center where the droplet is placed enters asymmetrically in the contact.

Fig. 9 also shows the results of the Wilson-Walowit film thickness equation, which in all cases corresponds better with the symmetric droplet trials than with the asymmetric droplet trials. In the case of droplet test 1 (where the symmetric experiment resulted in 50% lower film thickness) a very good agreement between the symmetric droplet trials and the Wilson-Walowit equation is observed. In the case of droplet test 2 the Wilson-Walowit equation underestimates less the experimental results for the symmetric droplet trials. It is expected that with a more precise mixed-lubrication model (such as described in [16]), the agreement between model results and symmetric droplet trials are even better.

From a lubrication viewpoint it is interesting to remark that according to Eq. (10), the slope of a curve through the data points in Fig. 9 is expected to be equal to 1. However, in Fig. 9 the slope is close to 0.7, a value that is commonly found in EHL-experiments (Montmitonnet [39]), highlighting the influence of elastic work roll deformation on the lubricant film thickness in cold rolling. Furthermore it is remarked that the inlet angle can also be varied by changing the thickness reduction in the rolling process. In Fig. 9b results are shown for a rolling force of 500 kN and a rolling force of 700 kN, resulting in a thickness reduction of approximately 3% resp. 10%. The lower the rolling force, the smaller the thickness reduction and inlet angle and therefore the thicker the resulting lubricant film. This relation, already experimentally observed by many other researchers (for example by Azushima [17], and Sutcliffe [18]), is consistently replicated in these experiments.

Table 2
relevant process, strip and oil parameters of the droplet trials.

Parameter	Value in first droplet test	Value in second droplet test
Rolling force, P	650 kN	700 kN and 500 kN
Entry thickness strip, t_{in}	1.40 mm	0.84 mm
Exit thickness strip, t_{out}	1.25 mm	0.76 mm when force is 700 kN and 0.81 mm for a force of 500 kN
R_a-value incoming strip roughness	0.3 μm	0.15 μm
Estimated flow stress, σ_{flow}	730 MPa	860 MPa
Oil type	Mineral oil	Fully formulated rolling oil
Oil base viscosity, η_0	0.058 Pa·s at 40°C	0.032 Pa·s at 40°C
Viscosity-pressure parameter, γ	$1.7{\cdot}10^{-8}$ Pa^{-1} at 40°C	$1.1{\cdot}10^{-8}$ Pa^{-1} at 40°C
Work roll radius, R_0	196.6 mm	196.6 mm
R_a-value work roll roughness	0.08 μm	0.08 μm
Entry/Exit tension, $\sigma_{entry}/\sigma_{exit}$	7.5 kN	7.5 kN
Rolling speed, v_{roll}	0.4–0.8 m/s	0.2 – 1.2 m/s
Strip width, b	100 mm	100 mm

4.3. Validation of theory for symmetric rolling process

If material didn’t pass over a guiding roll before being rolled, the asymmetric behavior was not observed. Fig. 10 shows a typical image of the reference process (with adapted contrast) together with calculated displacement and strain fields (the calculated fields are based again on 20 images).

The photo in Fig. 10 suggests that the process is symmetrical, nevertheless the calculated vertical displacement field and incremental strain field reveal some minor asymmetry. This asymmetry is much smaller than when the strip passed over a guiding roll (see for comparison Hoefnagels et al. [33] or the photo in Fig. 8). Therefore, such a rolling process will be called “symmetric” in the remainder of this article.

For the cold rolling processes considered in this work, the length of strip-roll contact divided by the strip thickness is greater than 3. According to Montmitonnet [21] a slab rolling model is accurate for such processes. In Fig. 10 it is shown that indeed the horizontal displacement gradients over the strip thickness are small. This supports the conclusion that a slab rolling model can be used to describe such rolling processes. However, a marked difference with the slab rolling model is that in Fig. 10 both the horizontal and vertical strip deformation starts before the roll bite entry.

In the photo and graphs of Fig. 10 the entry and exit of the roll bite are indicated as well. The contact length between strip and roll is

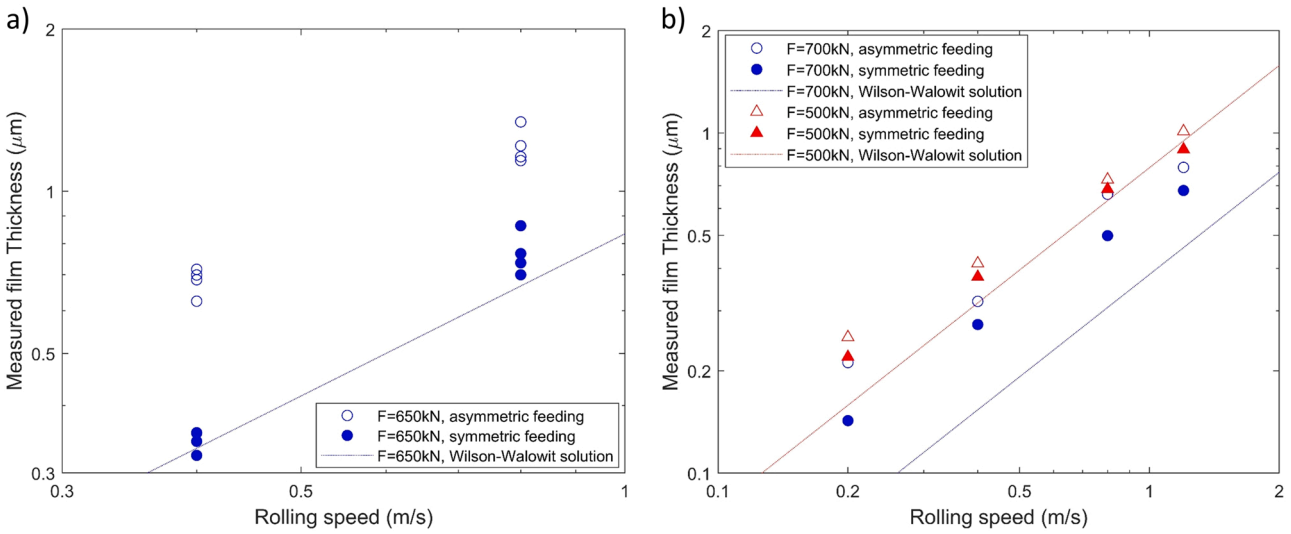

Fig. 9. measured oil film thickness (at the exit of the roll bite) with oil droplet method, both for symmetric and asymmetric strip feeding conditions, as a function of the rolling speed. a) droplet test 1, $t_{in} = 1.40$ mm, b) droplet test 2, $t_{in} = 0.84$ mm. Open symbols indicate asymmetric feeding conditions, closed symbols indicate the corresponding droplet measurements under symmetric feeding conditions.

another crucial parameter in a cold rolling model as it has a significant influence on the rolling force. The contact length has been determined following the procedure detailed in paragraph 3.4; in this paragraph the procedure to determine the position of the neutral point with IDIC has also been detailed. For all rolling processes, the measured contact length and position of the neutral point are compared with the theoretical values (combining Eqs. 1 and 2 for the contact length, or Eq. (4) for the neutral point position), the result is shown in Figs. 10 and 11.

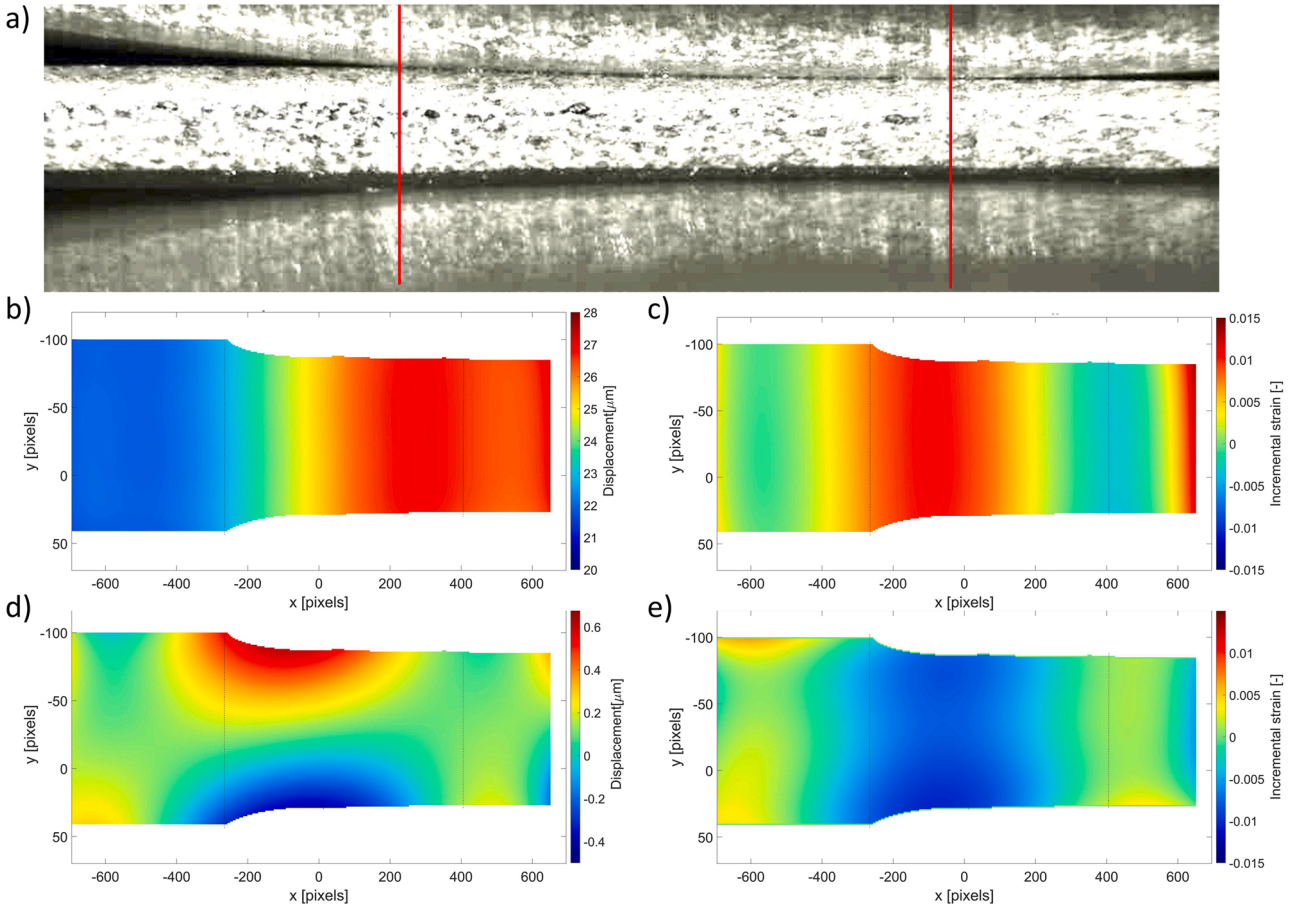

Fig. 10. results for the reference rolling process, with symmetric strip feeding conditions. a) photo of contact (contrast changed for clarity), with vertical lines indicating the entry/exit of the roll bite. b) measured horizontal displacement field. c) measured horizontal incremental strain field ($\Delta t \approx 0.04s$ as the frame rate of the camera is 25 s^{-1}). d) measured vertical displacement field. e) measured vertical incremental strain field.

Fig. 11 shows good agreement between the experimentally measured contact length and the theory. This means that the Hitchcock assumption is accurate enough to be used in combination with a slab-method to describe the cold rolling process. It was already reported before that the contact length can be accurately predicted by Eqs. 1 and 2. These results corresponds well with Li et al. [32] who only present DIC-results for one rolling process in which they also find a good agreement between the theoretical and measured contact length. Also Li et al. [24] report good agreement between theory and the contact length deduced from their partly rolled strips. Furthermore, Shigaki et al. [40] mention that as long as the deformed work roll radius is less than double the initial radius, the work roll deformation according to Eq. (1) corresponds well with more elaborate (Finite Element) models. In this work the deformed work roll radius is only 20–50% higher than the initial work roll radius.

However, it must be realized that Eqs. 1 and 2 assume ideal plastic (non-elastic) material behavior. In reality there will be an elastic recovery zone at the end of the roll bite and an elastic compression zone at the entry of the roll bite. The elastic recovery zone should make the total contact length longer than could be expected based on Eqs. 1 and 2. The good correlation between the experiments and the theory for rigid-plastic material behavior suggest that sink-in occurs at the entry of the roll bite (for the concept of sink-in see Oliver and Pharr [41]) and that the length of the zone where sink-in occurs must be approximately equal to the length of the elastic recovery zone.

Fig. 11 shows that when the neutral point is further from the entry, the IDIC methodology finds smaller values for $x_{NP,entry}$ than predicted by Eq. (4). Again this corresponds to results from Li et al. [32] who also find the measured neutral point position closer to the roll bite entry than the theoretical position of the neutral point. This discrepancy between theory and measurement of the neutral point position seems to be related to the observation presented in Fig. 10, that according to IDIC the deformation already starts before full contact with the work rolls has been established. Therefore, even before the roll bite the horizontal strip speed already increases and consequently at an earlier position it will match the work roll speed. This effect is not taken into account by the theory, where it is assumed that the material only starts deforming when it enters the roll bite. The question how realistic it is that plastic strip deformation occurs before the roll bite is addressed in the discussion.

5. Discussion

5.1. Accuracy of the IDIC-methodology

In this study conclusions are drawn from studying the edge of the strip. Cold rolling is primarily a plane strain process, but obviously at the strip edges the plane stress state prevails. The determinant of the deformation gradient tensor **F** is related to volume change via Eq. (6) and thus to the mode of deformation. For the reference case, the value of the determinant of **F** is calculated over the Region Of Interest (ROI) and plotted in Fig. 12.

At the very boundary of the ROI, $\det(\mathbf{F})$ significantly deviates from 1, which is an artefact of any DIC-method. Elsewhere, throughout the deformation region, the values for the determinant are close to 1, this is one of the checks to verify that the IDIC method has been correctly implemented. Furthermore it can be concluded that even at the strip edge, under plane stress condition, the deformation almost exclusively takes place in the rolling direction and the vertical direction.

Another point of discussion is that with the IDIC-method, horizontal and vertical strains are measured already before the strip makes contact with the work rolls. The strain values in Fig. 10 suggest that this deformation already exceeds the elastic limit, the question remains if this is realistic. As the true displacement fields in IDIC are approximated by polynomial functions, it is possible that a discontinuous vertical velocity change at roll bite is not captured accurately enough. Nevertheless it was verified that if higher order terms are allowed in the optimisation, the IDIC-results remain approximately the same, i.e. deformation starts well before contact with the work rolls is established. Furthermore, Fig. 12 shows that $\det(\mathbf{F})$ is very close to one in this region, suggesting that the IDIC-results are accurate there. Finally, careful examination of the photo in Fig. 10 also seems to suggest that the strip becomes already thinner well before contact with the work rolls occurs. This suggests that the deformation starts already before full contact with the work rolls is established.

In hot rolling, where the strip is thicker and the coefficient of friction is higher, the existence of a pre-deformation zone is generally accepted. Kim et al. [42] show how to take the existence of this zone into account for the calculation of rolling force. Ngo [43] shows with FEM that such a zone should also exists in (most) cold rolling processes and the current experimental results confirm this new insight. Because this pre-deformation zone has a significant influence on strip shape and profile [43], experimental confirmation of its existence is an important step to initiate further research in this topic. More DIC-experiments,

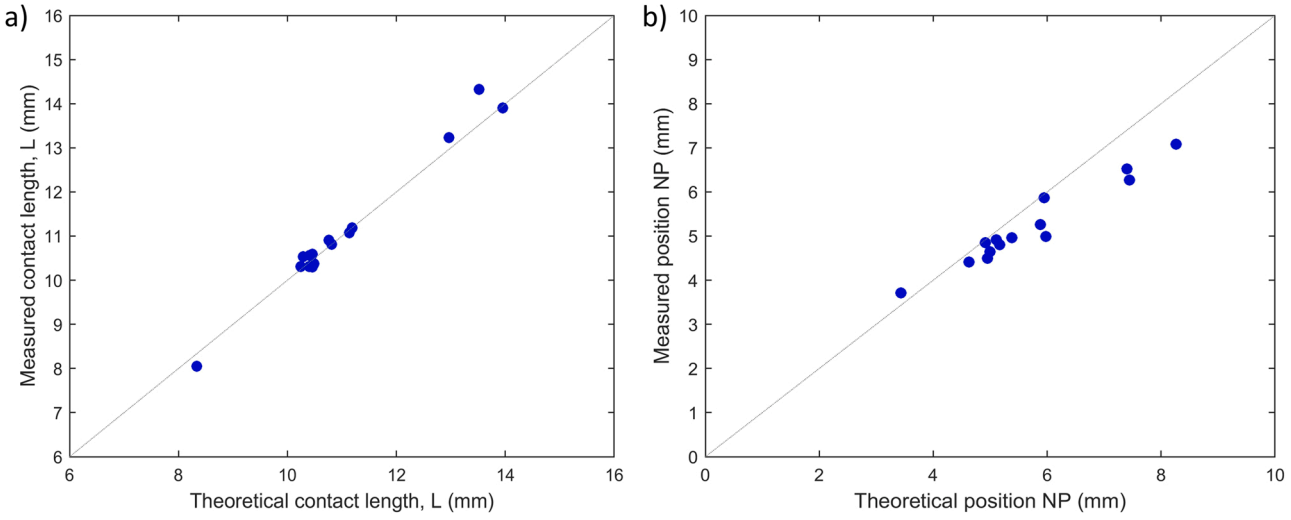

Fig. 11. a) comparison of measured contact length with Eq. (2) based on Hitchcock roll flattening (Eq. 1), b) comparison of the measured position of the neutral point with theoretical values obtained with Eq. (4). In both graphs, the dotted line indicates where theory exactly corresponds to measurement.

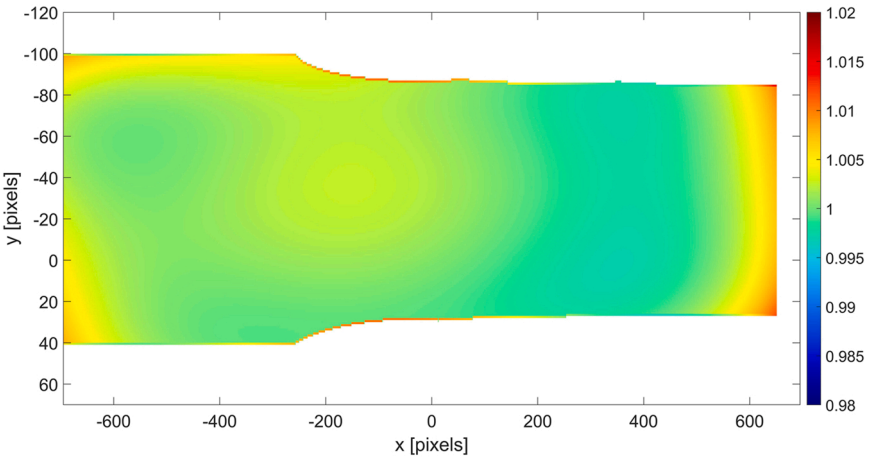

Fig. 12. determinant of the deformation gradient tensor in the ROI.

likely with improved cameras and comparison with FEM, would be necessary to determine the degree of plastic strip deformation in the zone before the strip makes contact with the work rolls and the impact this has on cold rolling models. Ngo [43] further mentions that on profiled strips "the center of the strip is in contact with the roll before the edges". The strips for the IDIC experiments were taken from the middle of a 1 m wide strip, therefore the profile over the final strip width of 100 mm is negligible. This mechanism described by Ngo can therefore not play a role in the IDIC experiments.

5.2. Root cause of asymmetric feeding in pilot mill

When material is passed over the guiding roll before being rolled, the strip feeding in the roll bite is asymmetric. Consistently the strip touches the upper work roll approximately 5 mm before it makes contact with the bottom work roll, this difference is significant as the total contact length is typically 10 mm. Fig. 8 also shows that the inlet angle with the top work roll is smaller than with the bottom roll. In all experiments the strip exits the roll bite in a symmetric way. The asymmetry appears to result from residual stresses induced by plastic bending of the strip over the guiding roll between the uncoiler and the mill stand. The top surface of the strip is elongated, while the bottom strip surface is compressed. After the guiding roll the applied strip tension forces the strip flat, resulting in a residual stress gradient over the strip thickness. This stress gradient can clearly be seen when cutting the strip between the uncoiler and the mill stand because the residual stresses will then relax resulting in a strip with downward bow.

According to (simple) theory, bending a tensionless strip results in plastic deformation when:

$$t_{in} > D \bullet \frac{\sigma_{flow}}{E_{strip}} \tag{11}$$

with D the diameter of the guiding roll, E_{strip} the Young's modulus of the strip material and σ_{flow} the flow stress of the strip material. Typical values for the parameters in the right hand side of this inequality, corresponding to the experiments, are: $D = 224mm, \sigma_{flow} \approx 400MPa$ and $E_{strip} = 210GPa$, these values suggest that plastic bending occurs for $t_{in} > 0.4mm$, so indeed for all trials described in this work. If strip tension is applied, plastic bending even occurs for (slightly) thinner strip gauges.

A suggestion for further research is to study how the material entrance is exactly affected by a certain distribution of residual stresses over the strip thickness. This could be investigated by accurate FEM cold rolling models.

Not only guiding rolls can be responsible for residual stresses in the strip, they can also be induced by previous process steps (pickling, slitting, coiling). Because the diameter of the guiding roll is small (and is positioned just before the roll bite), the guiding roll has the most significant contribution to the residual stresses. The impact of asymmetric strip feeding on the rolling process and the industrial relevance will be discussed further in Sections 5.3 and 5.4.

5.3. Impact of asymmetric strip feeding

The DIC experiments presented in paragraph 4.1 and 4.3 were carried out without lubrication. For dry rolling the impact of asymmetric feeding on the rolling parameters is limited. In contrast, industrial cold rolling processes are always lubricated and it is well known from Wilson and Walowit [9] that the thickness of the lubricant layer that is entrained in the roll bite depends on the inlet angle. It was therefore anticipated that the asymmetric feeding could have an influence on the lubricity and the experiments described in paragraph 4.2 were carried out to prove this. The impact of asymmetric strip feeding on lubrication is demonstrated in Fig. 9. Clearly the measured lubricant film is thicker when the material is fed asymmetrically in the mill. This corresponds with the expectations; the droplet is placed on the top strip surface and the photo in Fig. 8 show that the inlet angle with the top surface becomes smaller because of the asymmetry. Although in the asymmetric droplet tests the strip is initially not supported from the bottom, it follows from the results that this does not significantly influence lubricant film formation.

As shown in Fig. 9, the experimental film thickness can easily be 100% higher if the material entrance is asymmetric (compared to symmetric). Furthermore this figure shows that the film thickness difference between asymmetric and symmetric feeding is smaller for thinner strip. This is logical because the flow stress of thinner strip is higher because of work hardening and Eq. (11) indicates that plastic bending is less important for hard strip. Furthermore, in the experiments a constant tension force is applied, so the tension stress is higher for thin strip. Finally, also the strip stiffness decreases with its thickness, therefore thin strips will be pulled flat more easily than thick strips. For these reasons, for thinner strip the difference in inlet angle (between symmetric and asymmetric feeding) is smaller.

Mixed-lubrication models, commonly used to quantify the oil film thickness in cold rolling, always assume symmetric feeding conditions, therefore the possible effect of asymmetric feeding must be taken into account when validating any mixed-lubrication model with droplet measurements. Accurate quantification of the inlet angle is only possible if the strip truly symmetrically enters the roll bite, which is therefore a prerequisite for a meaningful experimental validation of mixed-lubrication cold rolling models. The procedure detailed in Section 4.3 can be used to achieve a perfectly symmetric material entrance.

Also other mechanisms can cause asymmetric lubrication in a rolling

mill. Notably oil falling from the bottom strip side because of gravity is another likely mechanism. Gravity favours lubrication of the top strip surface, but asymmetric material entrance could also favour lubrication on the bottom strip side if material passes under a guiding roll before being rolled. For some mills the lubrication efficiency is better on the bottom side, for this reason the authors suspect that the asymmetric feeding mechanism is relatively (much) more important than the influence of gravity. Another cause of asymmetric lubrication is that the residual stresses in the strip result in a gradient of horizontal tension over the strip thickness. According to Eq. (10) this leads to different lubricant film thickness on both strip surfaces. However, for common values of γ and σ_{flow} the entry tension only has a negligible influence on lubricant film thickness, certainly much smaller than the observed difference between symmetric and asymmetric strip feeding.

5.4. Relevance of asymmetric feeding for industrial cold rolling mills

Plastic strip bending over guiding rolls takes place also in industrial rolling mills, as before the first stand usually a guiding roll is used to bring the strip to the pass-line level. Therefore, in the first stand of an industrial mill this will lead to a difference in inlet angle according to the mechanism described in paragraph 5.2, but it could be argued that the influence on lubricant film build up is less as the process is still likely in the boundary lubrication regime. Another effect of the residual stresses, that will be more pronounced in the industrial mill where the strip is wider, is that it will result in crossbow (i.e. material bending in the width direction). This can give problems in the line because of the upstanding edge of the strip.

Plastic bending of the strip is also possible between later stands in an industrial tandem mill as commonly damming rolls and tensiometer rolls are placed between two rolling stands. Damming rolls are used to remove emulsion from the strip surface and tensiometer rolls are used to measure the strip tension. Fig. 13 schematically shows this configuration, it is possible that other rolls are present as well. Initial calculations show that despite the small contact angle with these rolls, plastic bending can occur (depending on the strip thickness). According to these calculations, the resulting residual stresses are significantly lower than in the pilot mill experiments, so the asymmetry will be less pronounced.

It is possible that industrial cold rolling defects are directly related to the asymmetric material entrance. Asymmetric lubrication in an industrial mill may influence rolling force, mill stability, surface aspect and bow problems, as described in the Introduction. The full impact of the observed asymmetry on the rolling process should be investigated in future research. According to Nakagawa et al. [44], heat scratches, a typical lubrication related problem at tin plate mills, occur mostly on the bottom side of the strip. This could suggest that lubrication is worse on the bottom strip side which is most likely due to asymmetric strip feeding.

6. Conclusions

IDIC was successfully applied to visualize the contact geometry and the velocity gradients in cold rolling. Cold rolling is a steady state process, therefore particle displacements are based on multiple image pairs. This significantly increased the accuracy of the method over a local DIC-method. The following conclusions can be drawn from the work presented in this article:

1. A novel finding was that despite using coils and applying entry tension, the strip still can enter asymmetrically in the rolling mill. It was shown that this is due to residual stresses resulting from plastic bending of the strip over a guiding roll. The degree of asymmetry depends on the process conditions and strip dimensions (especially entry tension and strip thickness).
2. Because of the strip curvature, the inlet angle at top and bottom work roll is not equal. As a consequence, due to a different inlet geometry, the hydrodynamic pressure build up is different. Droplet experiments have validated the effect of the inlet geometry on lubricant film thickness. A difference up to 100% in lubricant film thickness was measured between symmetric and asymmetric strip feeding. This effect of asymmetric feeding must be taken into account when validating a mixed-lubrication model with droplet measurements.
3. For a meaningful experimental validation of mixed-lubrication cold rolling models, a truly symmetrical rolling process is crucial. This work shows how a truly symmetrical rolling process can be achieved by assuring that the strip does not pass over any guiding rolls. For a symmetric rolling process the measured film thickness corresponds significantly better with the theory than for an asymmetric process.
4. For symmetrical cold rolling processes, the length of the deformation zone obtained with the camera validates the contact length based on the Hitchcock radius. The position of the neutral point determined with IDIC corresponds fairly well to the theoretical values. This can be explained by the observed plastic strip deformation before full contact between strip and work rolls has been established, which is not taken into account in the slab rolling model.

CRediT authorship contribution statement

L.J.M. Jacobs: Writing – original draft, Conceptualisation, Methodology, Investigation, Validation.' **K.N.H. van Dam:** Methodology, Investigation, Validation. **D.J. Wentink:** Writing – review & editing. **M. B. de Rooij:** Conceptualisation, Supervision, Project administration, Writing – review & editing. **J. van der Lugt:** Writing – review & editing, Project administration. **D.J. Schipper:** Writing – review & editing. **J.P. M. Hoefnagels:** Conceptualisation, Supervision, Project administration, Writing – review & editing.

Declaration of Competing Interest

The authors declare that they have no known competing financial

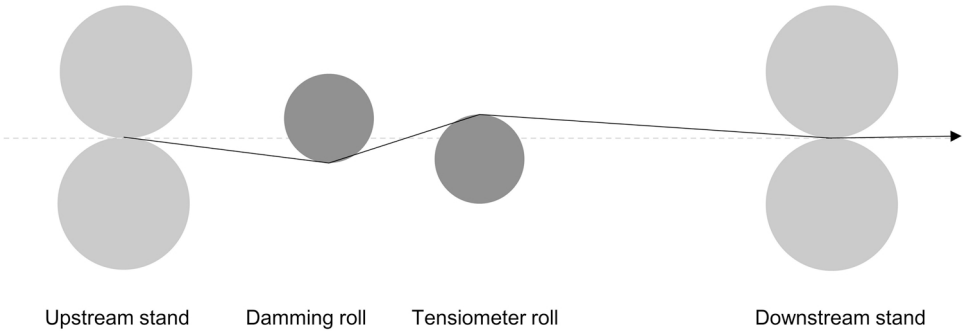

Fig. 13. schematic interstand strip movement in typical industrial mill.

interests or personal relationships that could have appeared to influence the work reported in this paper.

Data Availability

Data will be made available on request.

Acknowledgements

The authors kindly thank Tata Steel for permission to publish this document. Furthermore they like to thank Daphne van de Giesen, Hans Weel and Brian du Pont for their help in setting up the experiments and carrying out the pilot mill trials. The help of Erwin Spelbos with the camera and the technical support of Marc van Maris at the TU/e was greatly appreciated. This research did not receive any specific grant from funding agencies in the public, commercial, or not-for-profit sectors.

References

[1] Azushima A. Tribology in sheet rolling technology. Springe Int Publ AG Switz; 2016. https://doi.org/10.1007/978-3-319-17226-2.
[2] Roberts CD. Mechanical principles of rolling. Iron Steelmak 1997;vol. 24:123–4.
[3] Matthews DL, Yuen WYD. Minimising skidding in cold rolling. South East Asia Iron Steel Inst 2006;vol. 35(2):11–20.
[4] Mekicha M, de Rooij MB, Jacobs L, Matthews DTA, Schipper DJ. Understanding the generation of wear particles in cold rolling processes. Tribology Int 2021;vol. 155: 106789. https://doi.org/10.1016/j.triboint.2020.106789.
[5] Lu X, Sun J, Wei Z, Li G, Zhang D. Effect of minimum friction coefficient on vibration stability in cold rolling mill. Tribology Int 2021;vol. 159:106958. https://doi.org/10.1016/j.triboint.2021.106958.
[6] Jeng YR, Lee JT, Hwu YJ, Liu LC, Lu CY. Effects of operation parameters of cold rolling on surface finish of aluminium. Tribology Int 2020;vol. 148:106321. https://doi.org/10.1016/j.triboint.2020.106321.
[7] Nakhoul R. 2014. "Multi-scale Method for Modeling Thin Sheet Bukcling under Residual Stress – in the Context of Cold Strip Rolling", PhD-thesis, École Nationale Supérieure des Mines de Paris.
[8] Sun J, Yi M, Sun Q, Lu M. Experimental investigation of the relationship between lubricants' tribological properties and their lubricating performances in cold rolling. J Tribol 2014;vol. 136(3):034502. https://doi.org/10.1115/1.4026886.
[9] Wilson WRD, Walowit JA. An isothermal hydrodynamic lubrication theory for strip rolling with front and back tension. Tribology Conv, Inst Mech Eng, Lond 1971;93: 164–72.
[10] Atkins AG. Hydrodynamic lubrication in cold rolling. Int J Mech Sci 1974;vol. 16: 1–19. https://doi.org/10.1016/0020-7403(74)90029-0.
[11] Lugt P. 1992. "Lubrication in Cold Rolling – Numerical Simulation using Multigrid Techniques", PhD-thesis, University of Twente.
[12] Marsault N. 1998. "Modélisation du régime de lubrification mixte en laminage à froid", PhD-thesis, École Nationale Supérieure des Mines de Paris (in French).
[13] Wilson WRD, Sakaguchi Y, Schmid SR. A mixed flow model for lubrication with emulsions. Tribology Trans 1994;vol. 37(3):543–51. https://doi.org/10.1080/10402009408983327.
[14] Szeri A, Wang S. An elasto-plasto-hydrodynamic model of strip rolling with oil/water emulsion lubricant. Tribology Int 2004;vol. 37:169–76. https://doi.org/10.1016/S0301-679X(03)00046-X.
[15] Cassarini S. 2007. "Modélisation du film lubrifiant dans la zone d'entrée, pour la lubrification par émulsion en laminage à froid", PhD-thesis, École Nationale Supérieure des Mines de Paris (in French).
[16] Boemer D. 2020. "Numerical Modeling of Friction in Lubricated Cold Rolling", PhD-thesis, University of Liège.
[17] Azushima A. Determination of oil film thickness in rolling from the relationship between surface roughness of strip and roll. Bull JSME 1978;21(159):1402–7. https://doi.org/10.1299/jsme1958.21.1402.
[18] Sutliffe MPF. Friction and lubrication in metal rolling. Univ Camb 1989. https://doi.org/10.17863/CAM.14052. PhD-thesis.
[19] B.B. Aggarwal, W.R.D. Wilson 1978. "Thermal Effects in Hydrodynamically Lubricated Strip Rolling", Proc. 5th Leeds-Lyon symposium on tribology, I. Mech. E. paper X, pp. 351–359.
[20] Cuperus RS, ten Napel WE, Neumann WH, Smits RPJM. Measurements of film thickness and friction in cold rolling. Trans Mech Eng 2000;vol. 24(1):59–65.
[21] Montmitonnet P. Hot and cold strip rolling processes. Comput Methods Appl Mech Eng 2006;195:6604–25. https://doi.org/10.1016/j.cma.2005.10.014.
[22] Von Karman T. Beitrag zur theorie des walzvorganges. Z Angew Math Mech 1925; 5:139–41. https://doi.org/10.1002/zamm.19250050213.
[23] Sutcliffe MPF, Rayner PJ. Experimental measurements of load and strip profile in thin strip rolling. Int J Mech Sci 1998;40:887–99. https://doi.org/10.1016/S0020-7403(97)00138-0.
[24] Li L, Matsumoto R, Utsunomiya H. Experimental study of roll flattening in cold rolling process. ISIJ Int 2018;58:714–20. https://doi.org/10.2355/isijinternational.ISIJINT-2017-623.
[25] Siebel E, Lueg W. Untersuchungen Uber Die Spannungsverteilung Im Walzspalt. Mitt Aus Dem Kais-Wilhelm-Inst Eisenforsch Zu Düsseld, Book218 1933;15:1–14.
[26] Al-Salehi FAR, Firbank TC, Lancaster PR. An experimental determination of the roll pressure distributions in cold rolling. Int J Mech Sci 1973;vol. 15:693–700. https://doi.org/10.1016/0020-7403(73)90049-0.
[27] Weisz-Patrault D, Ehrlacher A, Legrand N. A new sensor for the evaluation of contact stress by inverse analysis during steel strip rolling. J Mater Process Technol 2011;211:1500–9. https://doi.org/10.1016/j.jmatprotec.2011.03.025.
[28] Carretta Y, Hunter AK, Boman R, Ponthot JP, Legrand N, Laugier M, et al. Ultrasonic roll bite measurements in cold rolling – roll stress and deformation. J Mater Process Technol 2017;249:1–13. https://doi.org/10.1016/j.jmatprotec.2017.05.036.
[29] Weisz-Patrault D, Maurin L, Legrand N, Ben Salem A, Ait Bengrir A. Experimental evaluation of contact stress during cold rolling process with optical fibre bragg gratings sensors measurements and fast inverse method. J Mater Process Technol 2015;223:105–23. https://doi.org/10.1016/j.jmatprotec.2015.03.047.
[30] Das S, Palmiere E, Howard IC. Effect of friction on deformation during rolling as revealed by embedded pin technique. Mater Sci Technol 2001;17:865–73. https://doi.org/10.1179/026708301101510654.
[31] Boldetti C, Pinna C, Howard IC, Gutierrez G. Measurement of deformation gradients in hot rolling of AA3004. Exp Mech 2005;45:517–25. https://doi.org/10.1177/0014485105059550.
[32] Li EB, Tieu AK, Yuen WYD. Application of digital image correlation technique to dynamic measurement of the velocity field in the deformation zone in cold rolling. Opt Lasers Eng 2003;39:479–88. https://doi.org/10.1016/S0143-8166(02)00030-1.
[33] Hoefnagels JPM, van Dam KNH, Vonk NH, Jacobs LJM. Accurate strain field measurement during strip rolling by exploiting recurring material motion with time-Integrated Digital Image Correlation. Exp Mech 2021. https://doi.org/10.1007/s11340-021-00781-y.
[34] Orowan E. The calculation of roll pressure in hot and cold flat rolling. Proc Inst Mech Eng 1943;150:140–67. https://doi.org/10.1243/pime_proc_1943_150_025_02.
[35] Johnson KL. Contact mechanics. Cambridge University Press; 1985.
[36] Jortner D, Osterle JF, Zorowski CF. An analysis of cold strip rolling. Int J Mech Sci 1960;2:179–94. https://doi.org/10.1016/0020-7403(60)90003-5.
[37] Hitchcock J. 1935. Roll Neck Bearings; Report of ASME Special Research Committee on Heavy-Duty Anti-Friction Bearings.
[38] Barus C. Isothermals, isopiestics and isometrics relative to viscosity. Am J Sci 1983; 45:87–96.
[39] Montmitonnet P. Modélisation du contact lubrifié — exemple de la mise en forme des métaux. Mécanique Ind 2000;1:621–37.
[40] Shigaki Y, Nakhoul R, Montmitonnet P. Numerical treatments of slipping/no-slip zones in cold rolling of thin sheets with heavy roll deformation. Lubrication 2015; vol. 3:113–31. DOI:0.3390/lubricants3020113.
[41] Oliver WC, Pharr GM. Measurement of hardness and elastic modulus by instrumented indentation: advances in understanding and refinements to methodology. J Mater Res 2004;19:3–20. https://doi.org/10.1557/jmr.2004.19.1.3.
[42] Kim YK, Kwak WJ, Shin TJ, Hwang SM. A new model for the prediction of roll force and tension profiles in flat rolling. ISIJ Int 2010;vol. 50(11):1644–52. https://doi.org/10.2355/isijinternational.50.1644.
[43] Ngo Q.T. 2015. "Thermo-elasto-plastic Uncoupling Model of Width Variation for Online Application in Automotive Cold Rolling Process", PhD-thesis, University of Paris-Est.
[44] Nakagawa K, Ito K, Yarita I, Kitamura K, Kitahama M, Kenmochi K, et al. Method of cold rolling oil evaluation in terms of heat streak resistance and strip surface cleaning property, together with their applications. Kawasaki Steel Tech Rep 1983; 7:55–67.